

Research Article

Research on Anchor Cable and C-Shaped Tube Support Method in Deep Layers Roadway, Experimental Study, and Numerical Simulation

Renliang Shan , Shupeng Zhang , Shengchao Xiao, and Junqi Liang

School of Mechanics and Civil Engineering, China University of Mining and Technology (Beijing), Beijing, China

Correspondence should be addressed to Shupeng Zhang; 782640988@qq.com

Received 9 September 2021; Accepted 25 September 2021; Published 11 October 2021

Academic Editor: Gan Feng

Copyright © 2021 Renliang Shan et al. This is an open access article distributed under the Creative Commons Attribution License, which permits unrestricted use, distribution, and reproduction in any medium, provided the original work is properly cited.

In roadways with high ground stress or burial depths, the joints distributed within rock formations are subject to complex stresses and interlayer misalignments frequently. Rock bolts and cable bolts anchored in the rock formations are subject to tensile and shear forces. Most of the bolts used in roadway engineering are local anchored, resulting in insufficient shear strength at the bolt free end close to roadway surface and increasing bolts breaking. The anchor cable and C-shaped tube (ACC) is a highly prestressed cable bolt that can withstand high shear force in its free end. This paper examines the effect of the relationship between C-shaped tube length and joint location on the shear resistance of ACC by double shear tests. To fully exploit the ACC's shear resistance, the C-shaped tube ends should be at least 30 cm beyond the joint. The effect of preload and concrete spray thicknesses on roadway deformation and plastic zone is investigated by numerical simulation. Results show that ACC and concrete spraying layer can form a stable extruded arch structure, so that the broken and soft rock within the loosen zone is in three-dimensional-stress state, effectively improving surrounding rock properties and controlling its deformation size. Based on these results, the ACC support design method is proposed.

1. Introduction

As coal resources are developed and exploration, many mines are gradually developing to depths of 1000 m and more, and deep roadways will face complex ground stress, water-rich, and other geological conditions, exhibiting obvious nonlinear large deformation characteristics [1]. When the roadway goes through formations, strength characteristics and hydrological behavior that affect the stability of the roadway are different. With the same method and strength of support as in normal roadways, the deep roadway will first be damaged in the local weak parts, and the local surrounding rock instability will aggravate the deformation and damage of other parts, which in turn will induce the overall disaster instability of the roadway [2–4]. Due to the poor interlayer cohesion, the low strength of the joint surface filler, and even gaps at the joints, not only are the deformation and strength of the joints clearly anisotropic, but also

the failure mechanism and mode are clearly different from other rock masses. With rock dip, weak surrounding rock, and high in situ stress, rock mass shows large loose zone and obvious asymmetric large deformation, which greatly increases the frequency of roof separation and interlayer misalignment. Most of the rock bolts and cable bolt currently used in roadway engineering are local anchor supports. As a result, the shear resistance of the bolt free end near the roadway surface is insufficient and the bolt breaking occurs frequently [5–8].

As an important means of geotechnical support, the support mechanism of bolt support is developed with the development of geotechnical support mechanism. There are two main modes of geotechnical anchoring mechanism and calculation model: one is the structural mechanics mode and the other is the geotechnical mechanics mode [9]. The geotechnical mode takes as its starting point the rock mass's own strength and its own load-bearing

capacity. This theory states that the role of the bolts is to reinforce the mechanical properties of the geotechnical mass and that macroscopically the bolts restrict the geotechnical mass by limiting it from its original position or producing large deformations, but mechanically they increase the shear strength features of the geotechnical mass [10–13]. It can be considered that the bolts and the geotechnical mass work together to form a strong composite system, advocating the full play of the surrounding rock itself as a support. Based on this theory, the loosen zone support theory is proposed. The loose zone support theory suggests that the rock will break and expand during excavation, and this deformation will produce a large or even larger load than the rock weight [14–17]. In deep roadways, there are mostly big loosen zone, and the support theory is based on the extruded arch and stresses protecting roadway surface by laying reinforcement mesh, shotcrete to prevent the surrounding rock from falling off in pieces, and forming an extruded arch structure with rock bolts and cable bolts, which will improve the shear strength parameters and control stability by extruding broken rock through pretension. Scholars studied experimentally the performance of bolts to strengthen joints. The experimental results prove that the stiffness and the peak shear strength of the joint bolted by prestressing bolts are higher than those of the joint bolted by bolts without preload. By increasing the preload, the range of prestress fields formed by the bolts is expanded. Overprestressed bolts can be susceptible to tensile damage, and the preload does generally not exceed half of yield load. Rock bolt's main body is a single solid steel bar with a low tensile strength, which limits the positive effect of pretension on improving the joint stiffness under shear. Cable bolts have a high tensile strength, but they are a flexible rigid bundle made up of multiple strands of steel strands, which have a low shear resistance. In order to overcome the shortcomings of cable and rock bolts, a support element named anchor cable and C-shaped tube (ACC) that can withstand high shear and axial force is invented. Scholars have studied the application methods of ACC in isolated working faces and through-layers roadways [18–20], but the influence of the relationship between the location of the C-shaped tube and the joint on the joint shear strength, the difference between high preload ACC and normal bolt, and the role of concrete layer on the extruded arch structure are not clear. In this paper, the relationship between the location of the C-shaped tube and the joint surface is investigated through double shear experiments, the design guidelines for the C-shaped tube length in the support design are determined, and the influence of the preload and concrete spray layer thickness on the plastic zone of the roadway is investigated through numerical simulations. Based on the research results a design method for the ACC support scheme is proposed.

2. ACC Introduction

The ACC is a highly prestressed cable bolt that provides a highly shear resistance in the free end (Figure 1). ACC adds a

C-shaped tube to the outer side of the cable bolt (Figure 2). C-shaped tube is a steel tube with a 15° straight gap on the side [21].

After ACC is installed, the bolt hole gradually deforms and squeezes the C-shaped tube, which shares the normal force for the cable bolt (Figure 1(b)). After the C-shaped tube shares part of the normal load, the cable bolt is subjected to a lower normal force than when there is no C-shaped tube, and the cable bolt can better perform its high tensile strength. The experimental results showed that the maximum axial force at the time of bolt damage was greater with the addition of the C-shaped tube than without it.

3. C-Shaped Tube Length

This experiment investigates the effect of the relationship between the location of the C-shaped tube end and the joint on the joint shear strength. The test table used to perform this experiment is shown in Figure 3. The preload was not applied on either side of the concrete blocks and a gap was left between the concrete blocks to eliminate friction [22]. Joints' shear strength is afforded by bolt shear and axial force in joints' direction. Unlike normal test tables, pure shear test tables highlight the shear resistance of the bolts and are more suitable for studying the shear resistance of comparative support elements.

In these tests, the shear strength of the joint was compared for four positions: C-shaped tube 30 cm from the joint, C-shaped tube just reaching the joint, C-shaped tube 15 cm beyond the joint, and C-shaped tube 30 cm beyond the joint. As the test table is a double shear test table, all C-shaped tubes are arranged symmetrically on both joints and keep the same opening direction.

3.1. Concrete Blocks Casting. Firstly, the concrete blocks were $300 \times 300 \times 300 \text{ mm}^3$ in size and poured in molds. Before pouring, an oiled steel pipe, with an external diameter of 32 mm, was placed in the molds holes to make a bolt hole. Use concrete grade C42.5 cement and stones with 10 mm–20 mm particle size to make concrete with strength of 40 MPa. Then, molds were coated with oil on the inner walls the mixed concrete is placed in the mold, and shake sufficiently to eliminate the pores. Flattening the upper surface of the concrete block ensures constant forces between the shear box and the concrete block. The poured concrete blocks were left indoors for 24 hours before the molds were removed and the strength reached 40 MPa after curing for 28 days (Figure 4).

3.2. Bolt Installation. The concrete blocks were packed into shear boxes before the experiment and three shear boxes were bolted together (Figure 5). The shear boxes are molds made of special steel and are wrapped around concrete blocks except for the joints and the outer sides.

The concrete blocks on both sides are placed on the metal tables. The cable bolts pass through concrete blocks, and both ends are fixed on the test table. The C-shaped tube opening direction affects the closure process. Before the

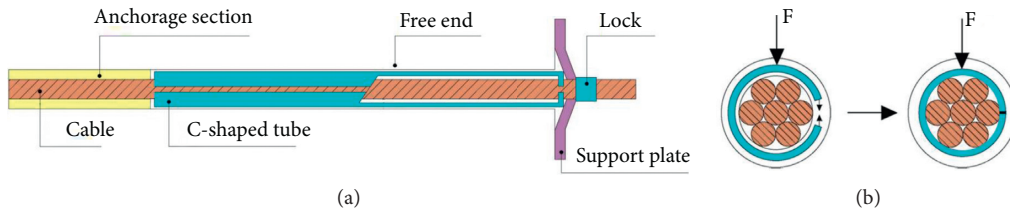


FIGURE 1: Schematic image of ACC structure and forced deformation. (a) Structure schematic diagram. (b) Deformation diagram under shear.



FIGURE 2: Physical view of ACC.



FIGURE 3: Double shear test table.

experiment, the C-shaped tube opening was 90° to the shear direction. To simulate the cable bolt free end, there was no infill between all cable bolts and the hole wall.

3.3. Double Shear Experimental Process. Before the experiment, control the right horizontal loading end to apply preload to the cable bolt. After reaching the target preload, keep the loading position unchanged until the end of the experiment. Start the shear experiment after removing the bolts connecting shear boxes. Then control the middle vertical loading end to contact the upper surface of the middle shear box, and start vertical loading. The loading rate is 2 mm/min, and stop the experiment after loading to damage. The maximum vertical load of the test bench used in this experiment is 600 t, and the maximum shear displacement is 200 mm. Axial force, normal force, and shear displacement during the experiment are imported into the computer by the sensor to generate real-time data.



FIGURE 4: Poured concrete blocks.

3.4. Experimental Materials. Double shear tests were performed on cable bolt and ACC using the shear test table described above. The experimental materials consisted of the same diameter cable bolt and ACC (Figure 6). The difference between ACCs was the C-shaped tube length.

3.5. Experimental Results. In these experiments, the variations of the shear capacity of ACC were investigated for four

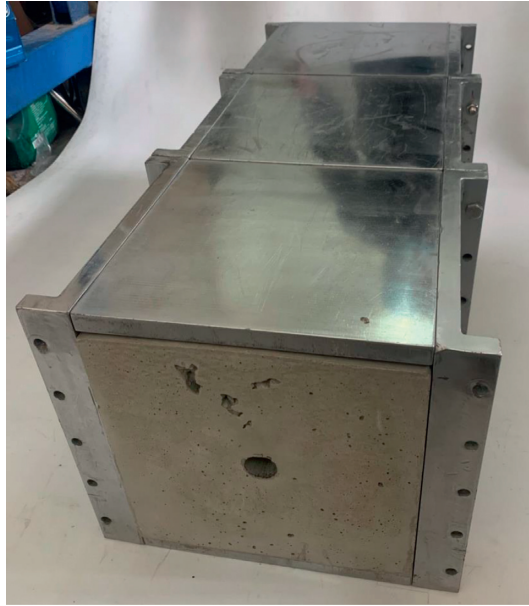


FIGURE 5: Concrete blocks in shear boxes.



(a)



(b)

FIGURE 6: Specimens used in experiments. (a) ACC and cable bolt (1.44 m). (b) C-shaped tube.

different positions of the C-shaped tube and the joint. With a hole length of 300 mm in a single concrete block, when the C-shaped tube is more than 30 cm from the joint surface, the test result in this condition was replaced by cable bolt. ACC was used to represent the experimental results when the C-shaped tube was more than 30 cm beyond the joint. Cable bolts diameter is 21.6 mm and C-shaped tubes have 28 mm outer diameter and 24 mm inner diameter. All bolts were loaded to damage and broke near joints (Table 1 and Figure 7).

The axial and shear forces follow the same trend as the shear displacement in four conditions. At the beginning of shear, there will be a period of slip stage of the joint, at this point there is no contact between the bolt and the hole wall, the bolt is unable to provide shear resistance and the joint shear strength is zero (Figure 8). As the shear displacement increases, the cable bolt or C-shaped tube contacts the hole wall, the shear force starts to increase, and there will be a section of nearly straight line, which is the high stiffness stage. Starting from the cable bolt contacting the hole wall, the concrete is crushed and broken by the cable bolt, and the curve begins to show small sudden drops.

The four curves show the same trend before the damage of the cable bolt, but the difference is the length of the slip stage and the joint peak shear strength. When the C-shaped tube reaches the joint, the joint shear strengths of ACC and cable bolt are basically equal, and the C-shaped tube only affects the length of the slip stage. It does not affect joint shear strength during shearing process and peak shear strength. When the C-shaped tube length rises over 30 cm beyond a joint, the slip stage was shortest and the joint shear strength during shear was significantly higher than other lengths, but the peak shear strength was the same as that of ACC with C-shaped tube 15 cm beyond the joint.

The relationship between the C-shaped tube length and the position of the joint has a significant impact on ACC's shear strength. As C-shaped tube length gets longer, slip state gets shorter. Before the C-shaped tube reaches the joint, the C-shaped tube length only affects the length of the slip stage. After the C-shaped tube length exceeds 15 cm of the joint, continuing to increase the C-shaped tube length does not affect peak shear load, but only improves shear strength during shear. To ensure the shear resistance of ACC, the C-shaped tube should be at least 30 cm beyond the joint when setting up the ACC support scheme.

4. Preload and Concrete Spray Layer Thickness

For the working condition of the original segment of a mine through-seam roadway, an analytical model was created for comparing different preloads on ACC and concrete spray layer thickness on the roadway deformation and plastic zone. The surrounding rock contains various conditions such as soft coal seam, stable rock formation, and rock inclination, which are used to test the support performance (Table 2). Analytical model length was 40 m, width was 3.2 m, and height was 45 m (Figure 9).

A 16.39 MPa uniform load is applied to the model's top to replace the self-weight stress of the overlying rock layers

in the original segment. Use the Mohr–Coulomb model for rock formations, cable elements for cable bolts, pile elements for C-shaped tubes (Table 3), beam elements for reinforcing trapezoidal beams, and shell elements for the reinforcing mesh and concrete spraying layer (Table 4). All rock formations have a dip of 15°.

The support was designed with ACCs, reinforced trapezoidal beams, reinforcement mesh, and shotcrete (Figure 10). The distance between two support sections was 800 mm. The ACCs of each section were connected by reinforced trapezoidal beams. Roadway surface was sprayed with 25 MPa concrete of 20 cm thickness.

4.1. Concrete Spraying Layer Thickness. The concrete spray layer prevents the surface layer of surrounding rock from falling out, restricts it from being extruded, keeps the internal rock in triaxial-stress state, and improves mechanical properties and stability of roadway.

Concrete spraying layer maintains extruded arch integrity. Four different thicknesses concrete spray layers were set up to observe their effects on plastic zone distribution (Figure 11).

Under these geological conditions and support conditions, the plastic zone is mainly distributed in the two sides, the bottom corner, and the shoulders. The plastic zone in the shoulder exhibits the characteristic of covering soft rock layers along the rock joint. The plastic zone in the left and right shoulders near the surface decreased significantly after increasing the concrete spray layer thickness, but the plastic zone in the deeper part of the surrounding rock remains unchanged. The preload force applied to the free end with a length of 1.8 m cannot be diffused to the deep rock mass. Under the action of the extruded arch consisting of concrete spray layer and highly prestressed ACCs, the fractured rock within loosen zone is in triaxial-stress state and exhibits better properties. ACCs arranged in soft rock formations require longer cable bolt lengths to increase the prestress diffusion range. This extruded arch structure is more effective for weak and fractured surrounding rocks and is not effective for complete and hard rocks. The soft surrounding rock here is not only the rock formation with poor mechanical parameters, but also the surrounding rock that shows soft rock properties under high ground stress. The concrete spraying layer is suitable for the roadway with large burial depth and high ground stress.

4.2. Preload. The preload influence on cable bolts and ACCs shear resistance was studied by double shear experiments, while concrete strength averaged 30 MPa [20].

The experimental results show that ACC has a higher shear resistance than cable bolts at any preload force (Table 5). Increasing the preload can reduce both cable bolt and ACC peak shear loads. When the preload is too high, the shear resistance of cable bolts will be significantly reduced, while ACCs still have high shear resistance at higher preload. Higher preload applied to ACC can exhibit better shear resistance.

TABLE 1: Double shear tests results.

Bolt type	Distance between C-shaped tube and joint (cm)	Peak shear load (kN)	Peak axial load (kN)	Displacement at failure (mm)
Cable	-30	636	431	78
ACC	0	643	434	82
ACC	+15	833	457	96
ACC	+30	836	443	77

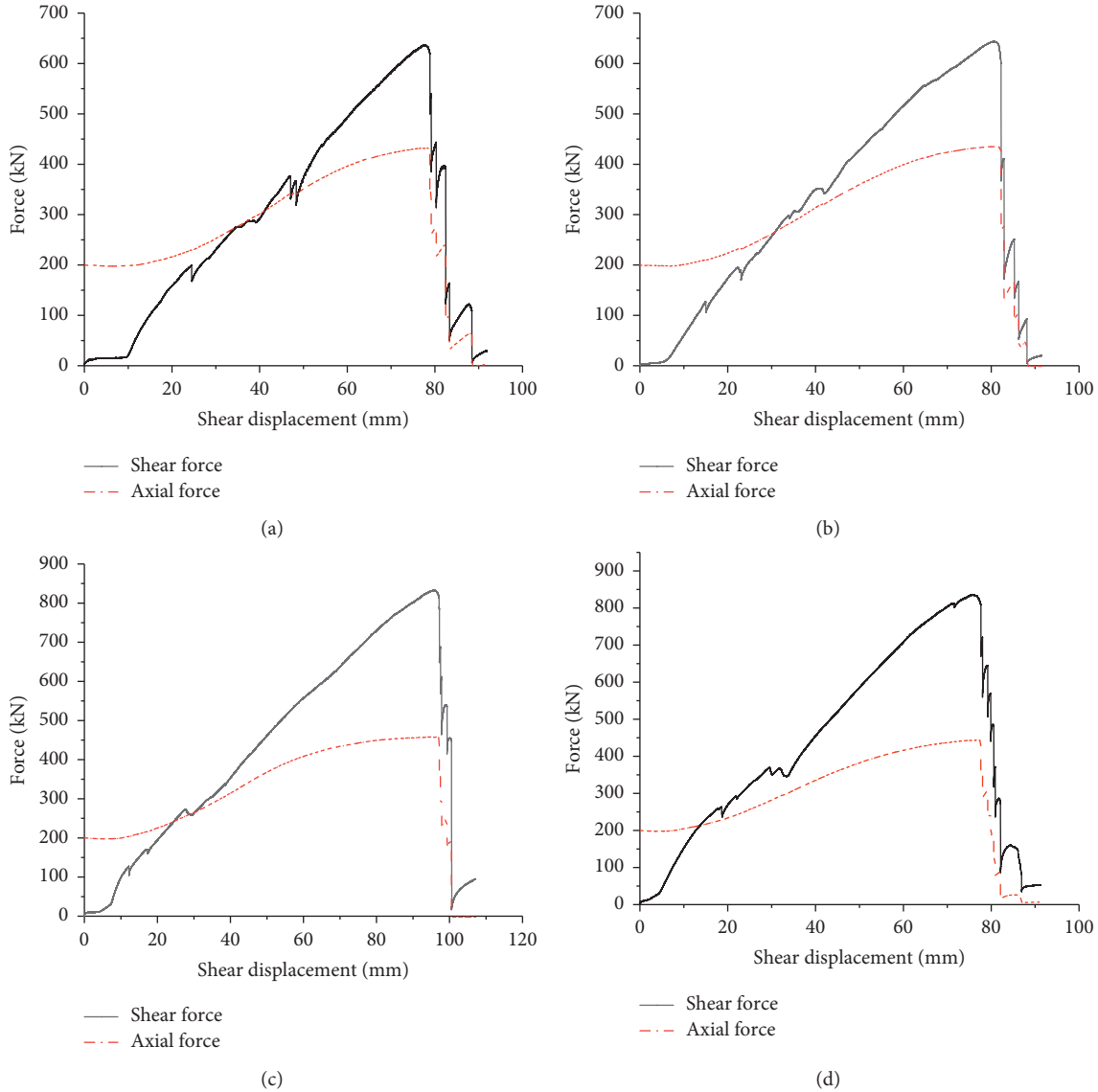


FIGURE 7: Force-shear displacement diagram of cable bolts and ACCs in shear process. (a) Distance = -30 cm. (b) Distance = 0 cm. (c) Distance = +15 cm. (d) Distance = +30 cm.

The roadway deformation is compared using the ACC support scheme when the roadway is at the joint between soft and hard rock. The number simulation uses the support method in Figure 9, with a concrete spray layer thickness of 20 cm and preloads of 0, 100, 200, and 300 kN.

Roadway deformation asymmetry due to soft rock layers and rock dip (Figure 12). Under unsupported conditions, the position of the largest horizontal displacement is in the coal seam of both shoulders, and the deformation range is

related to the joint between rock layers. To the vertical displacement, the roof sinking is influenced by the rock dip with larger value on the left side, and the floor is a whole rock layer with more symmetrical displacement.

When ACC support is used, the soft rock deformation in the deep layer roadway is controlled under the action of the extrusion arch. The deformation of both shoulders is obviously reduced, and the roadway deformation tends to be uniform.

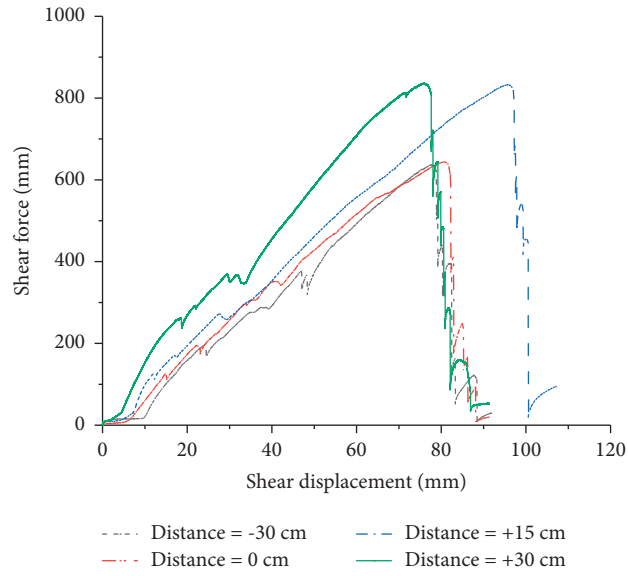


FIGURE 8: Shear force-shear displacement diagram with different positions between C-shaped tube and joint.

TABLE 2: Rock formation's parameters.

Rock layer	Gravity (kg/m ³)	K (GPa)	G (GPa)	c (MPa)	φ (°)	σ_t (MPa)
Coal	1500	2.8	1.6	0.5	23	0.7
Mudstone	2550	4.3	2.5	1.4	33	1.4
Sandy mudstone	2600	5.8	3	1.8	31	0.9
Middle sandstone	2650	6	3.6	3	35	2.1

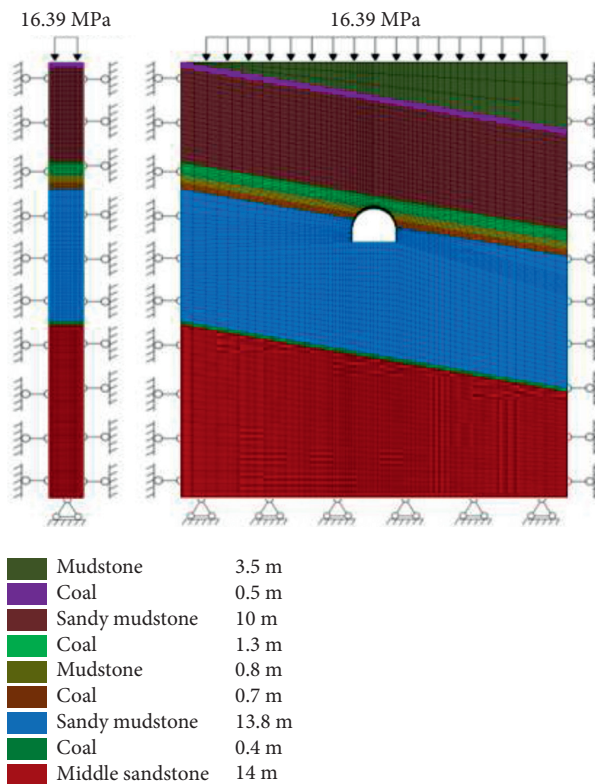


FIGURE 9: Model boundary conditions.

TABLE 3: Pile element parameters.

Type	E (GPa)	ν	A (mm ²)	ρ (mm)	k_n (MPa)	c_s (MN/m)	k_s (MPa)	c_n (MN/m)	Φ_s (°)
Pile	250	0.37	3.88e4	100	12	12	12	0	23

TABLE 4: Structural unit parameters.

Category	Cable	Beam	Shell
Diameter (mm)	21.6		
Cross-sectional-area (mm ²)	366	307.7	
Young (GPa)	195	200	26
Break load (kN)	450		
Grout-per (mm)	100		
Grout-sti (MN/m ²)	17.5		
Grout-coh (MN/m)	0.44		
Poisson's ratio		0.3	

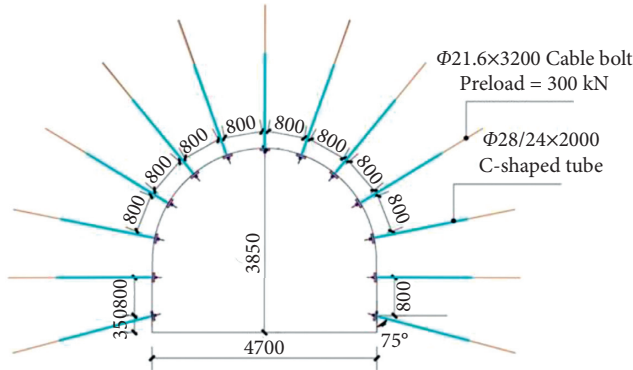


FIGURE 10: ACC support scheme (mm).

When the preload is different, the largest horizontal displacement is concentrated around left side and right shoulder, and right shoulder deformation is larger than left side. The vertical displacement is symmetric. Roof deformation is larger than floor. The horizontal and vertical displacements under different preload conditions are summarized in Table 6.

From Figure 12 and Table 6, the coal layer deformation is effectively limited by ACC support method. Increasing the preload can effectively control horizontal displacement. Compared with no preload, the displacement of both sides was reduced by 3.36%, 8.58%, and 12.42% when the preload was 100, 200, and 300 kN. The preload has less effect on controlling vertical deformation, and the reduction in vertical displacement is less than 2% at preloads of 100, 200, and 300 kN. The extruded arch structure of ACC can effectively control soft surrounding rock deformation. Preload applied to ACC is more effective in controlling horizontal displacement.

5. ACC Support Design Method

According to results of double shear experiments, numerical simulations, and extruded arch theory, ACC support design method is established after clarifying the effects of C-shaped tube length, prestressing, and concrete spraying layer

thickness on ACC resistance to shear load and reinforced surrounding rock.

ACC support is mainly targeted at the phenomenon of big loosening zone. Determine rock layer distribution around the roadway by borehole peeping and C-shaped tube and cable bolts length based on the rock layer distribution. Determine the geological conditions around the roadway through in situ stress test and surrounding rock mechanical property test. Select reasonable concrete spraying layer strength and thickness through numerical simulation. Finally, ACC and concrete spray layer can form a stable extruded arch structure.

The prestress of ACC spreads into a tapered area and squeezes loosen rock within that range. After selecting a suitable spacing, the tapered areas are connected to cover the fractured rock around the roadway. Regardless surrounding rock is broken or not, after reinforcing the surface surrounding rock through surface protection measures such as steel mesh and shotcrete to limit it from falling out and block extrusion, the rock inside the loosen zone will be in triaxial-stress state. The design process is shown in Figure 13.

Select suitable measurement points in the target roadway to measure the in situ stress around roadway. The relationship between the maximum principal stress inclination and maximum principal stress direction and the relationship between horizontal and vertical stresses have significant effects on the roadway deformation. Then cores were taken from holes drilled at the roadway and brought back to the laboratory for mechanical property testing to determine the surrounding rock parameters. Next, holes were drilled in the two sides and roof of the roadway, not less than 5 m in the two sides and 8 m in the roof. Borehole peepers were used to observe the relationship between rock layers around the roadway and the range of loosen zone.

The key to the design is in the selection of the appropriate cable bolt length (L_b), the C-shaped tube length (L_c), and the concrete spray layer thickness. L_b is dependent on loosen zone thickness, soft rock, and distance to the stable rock formation. When there is soft rock in the surrounding rock, L_b needs to be extended to expand the prestress diffusion range. According to the loosen zone theory, the extruded arch thickness (T_a) is determined by

$$T_a = \frac{L_b \times \tan \theta - S}{\tan \theta}, \quad (1)$$

where θ is control angle of bolts to rock mass, commonly taking the value of 45°, and S is bolts spacing. Select the appropriate cable bolt length so that T_a is greater than loosen zone range. When there is a stable rock layer near the roof, L_b needs to be extended to the stable rock layer.

L_c should be at least greater than the loosen zone thickness. When there is rock intersection or joints in the deep surrounding rock, and interlayer misalignment has

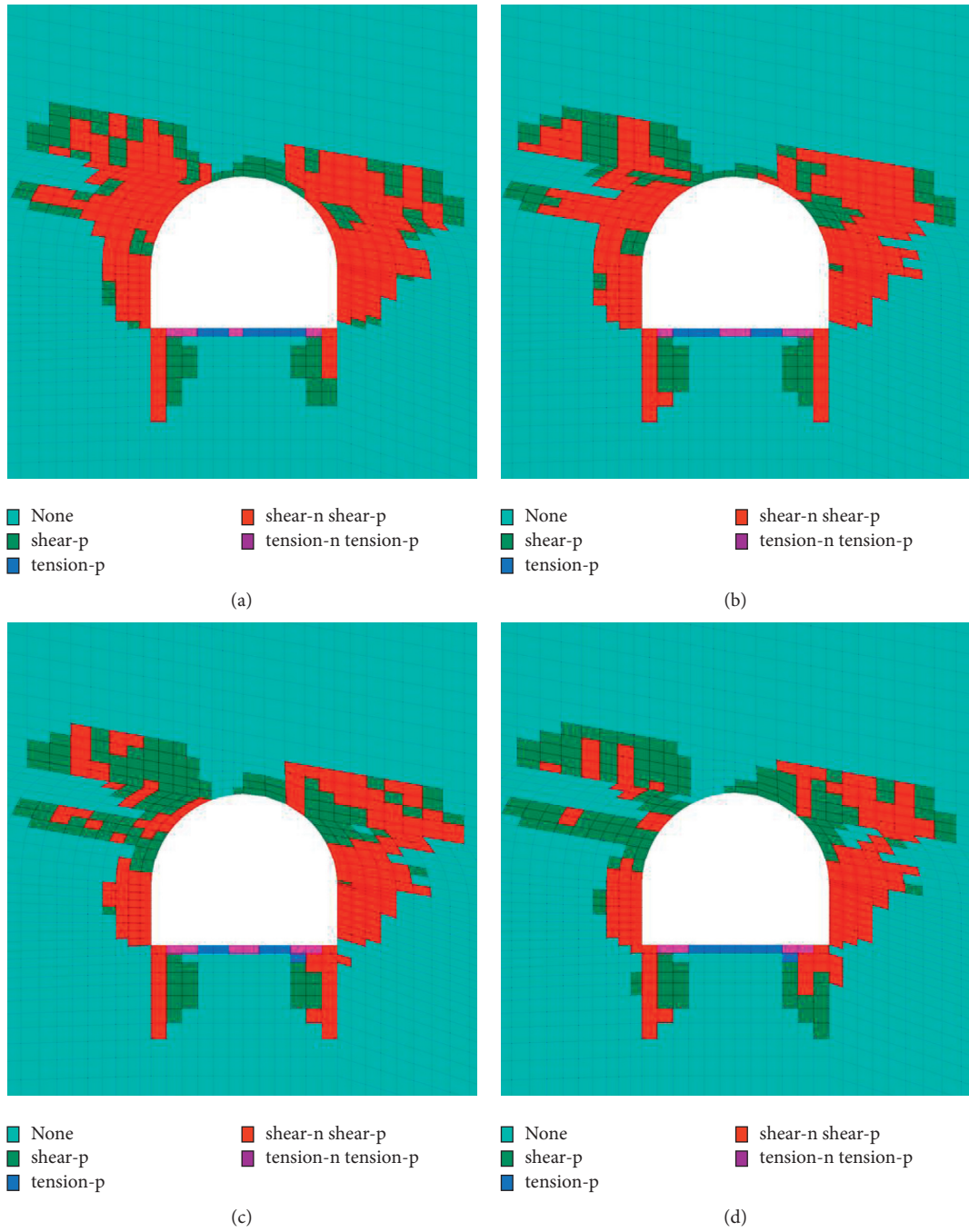
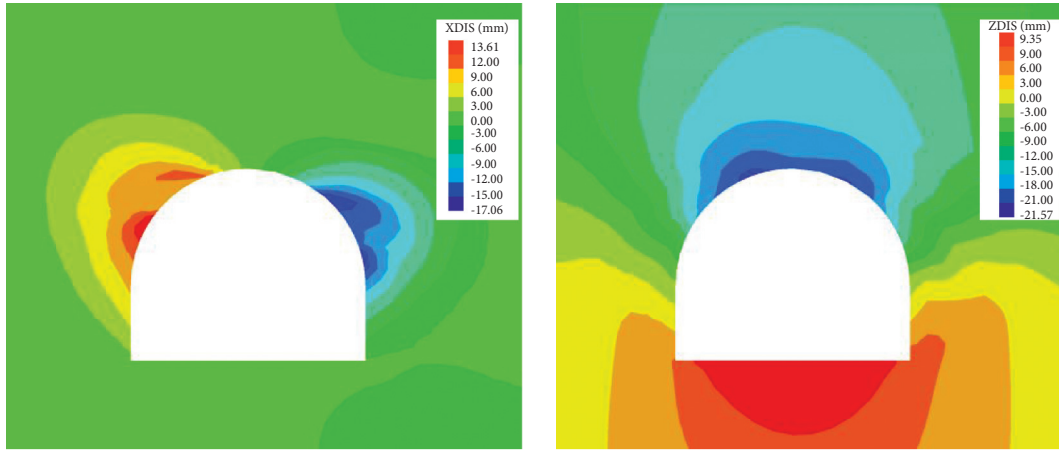


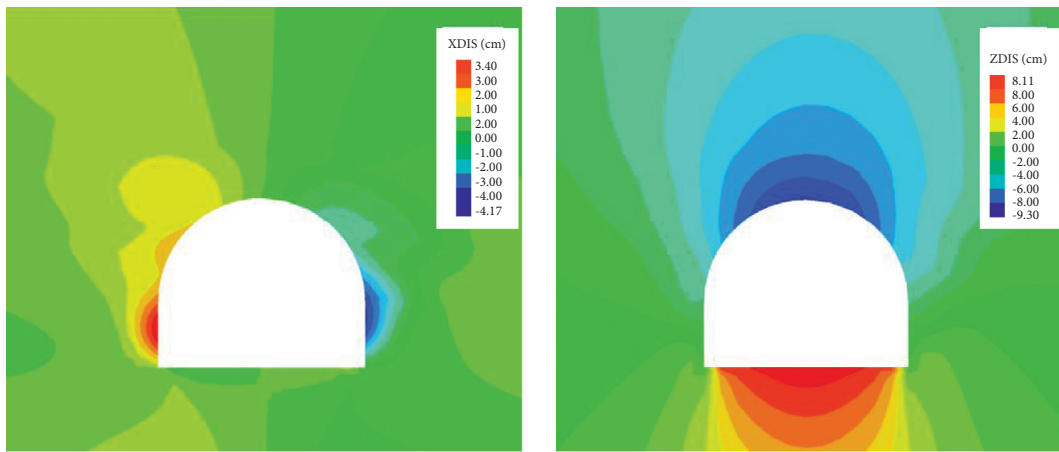
FIGURE 11: Distribution of plastic zone with different thickness of concrete spraying layer. (a) Thickness 15 cm. (b) Thickness 20 cm. (c) Thickness 25 cm. (d) Thickness 30 cm.

TABLE 5: Test results of cable bolts and ACCs under different preloads.

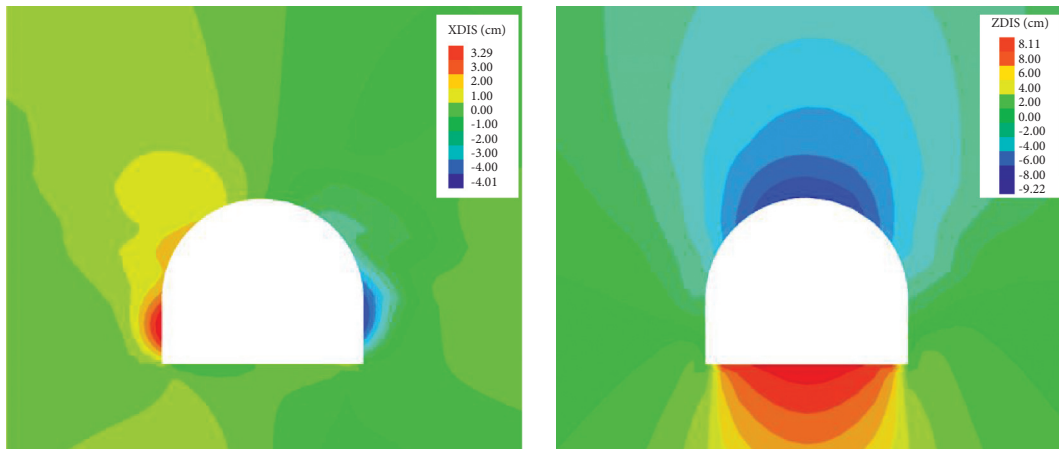
Bolt type	Preload (kN)	Peak shear load (kN)	Peak axial load (kN)	Shear displacement at failure (mm)	Peak shear load reduced ratio (%)
Cable	100	627	419	106	
Cable	200	605	438	97	3.5
Cable	300	560	435	97	10.7
ACC	100	818	459	120	
ACC	200	813	459	126	0.6
ACC	300	791	467	104	3



(a)



(b)



(c)

FIGURE 12: Continued.

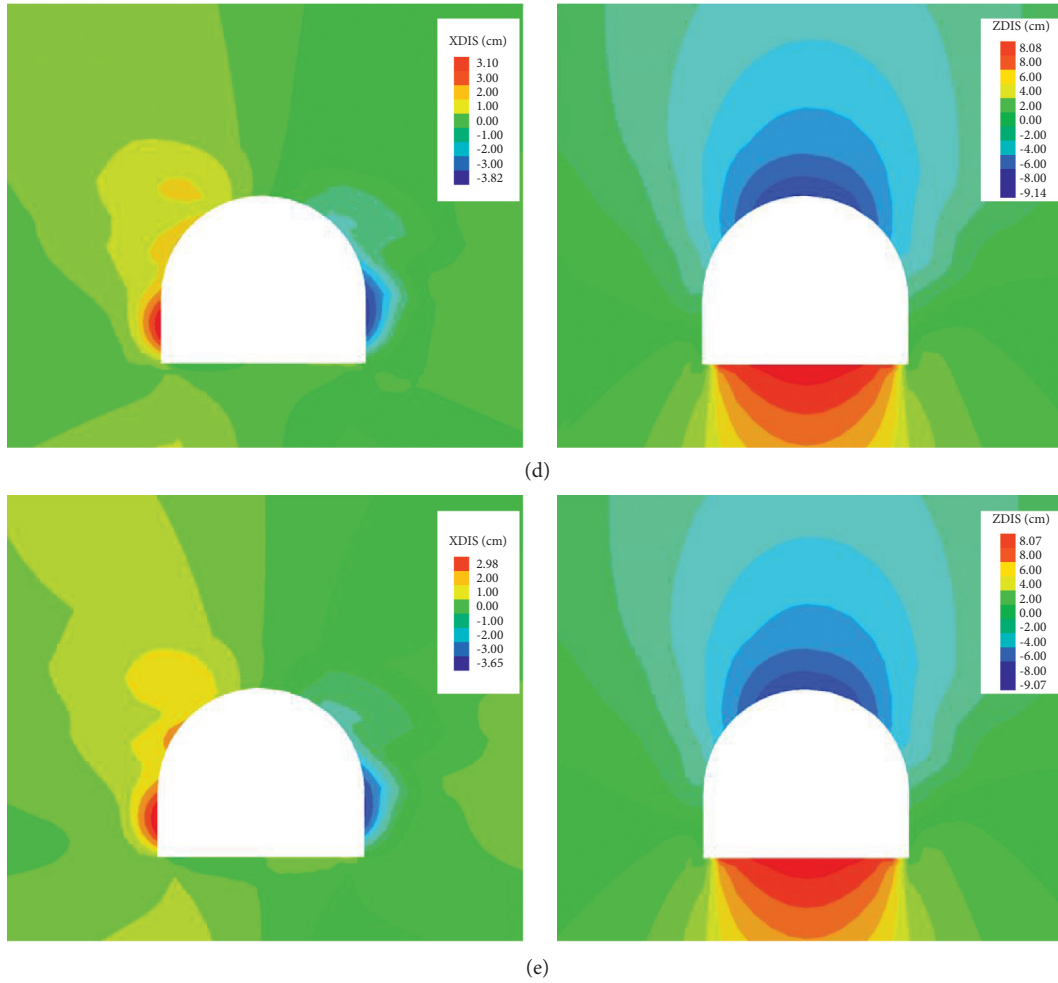


FIGURE 12: Deformation condition of the roadway with different preload forces (horizontal displacement on the left; vertical displacement on the right). (a) No support. (b) preload = 0 kN. (c) preload = 100 kN. (d) preload = 200 kN. (e) preload = 300 kN.

TABLE 6: Deformation of the roadway under different preload conditions.

Preload (kN)	Left side deformation (mm)	Right side deformation (mm)	Roof deformation (mm)	Floor deformation (mm)	Two-side movement (mm)	Roof-floor movement (mm)
0	34	41.7	93.0	81.1	75.7	174.1
100	32.9	40.1	92.2	81.1	73.0	173.3
200	31.0	38.2	91.4	80.8	69.2	172.2
300	29.8	36.5	90.7	80.7	66.3	171.4

occurred or may occur under the engineering disturbance, L_c needs to be extended to the joint, and at least a certain length beyond the joint to ensure that ACC can function effectively as a shear resistance. L_c is related to loosen zone thickness, potential slip joints, and distance between joints and roadway surface, as in

$$L_c = \max\{L_z, L_d + L_s\}, \quad (2)$$

where L_z is loosen zone thickness; L_d is distance between the roadway surface and rock interfaces or large joints; L_s is the length to ensure the shear strength of ACC, at least taking 30 cm. When L_c is less than or equal to L_d , ACC does not have high shear resistance.

W-steel strip and reinforcing mesh are necessary components in the support design. W-steel strip balanced forces of ACCs in the same section, prevents cable bolts from breaking in the stress concentration area, and has a certain role in surface protection. The reinforcement mesh is a necessary surface protection measure that restrains the rock radially along the roadway. In support design, ACC is used in the whole section of the roadway. ACC preload should not be less than 300 kN, and ACC preloads in the two sides are higher than the roof. W steel strip connects ACC and presses reinforcement mesh on the roadway surface. For the roadway with loosen zone thickness more than 150 cm, it is necessary to spray

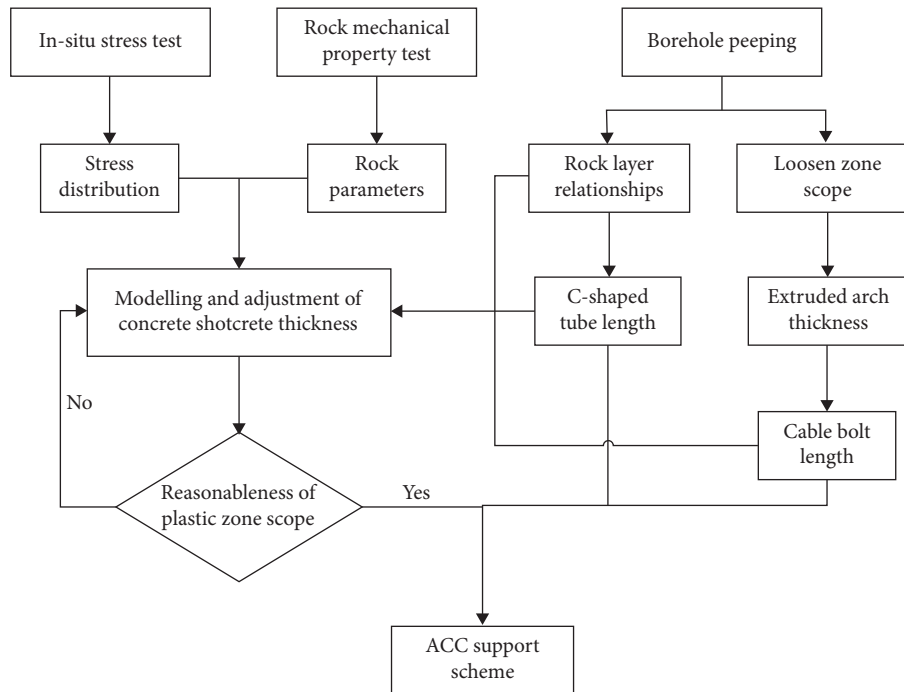


FIGURE 13: ACC support design process.

concrete on the roadway surface, and the concrete strength should not be less than C25.

Correction of the actual thickness of the rock layers around the roadway in relationship of the rock layers is obtained from the borehole peeping, and the rock layers parameters are obtained from mechanical properties testing. Numerical modelling was established in the fast Lagrangian differential analysis software Flac^{3D}. Adjust the strength and thickness of the concrete spray layer to a significantly reduced extent of the plastic zone around the roadway and have a partial safety allowance.

Finally, based on the concrete spray layer parameters obtained from the numerical simulation, the ACC support scheme was obtained by combining the cable bolt length and the C-shaped tube thickness.

6. Conclusions

The key to the ACC support design is in the selection of the appropriate cable bolt length, the C-shaped tube length, and the concrete spray layer thickness. The relationship between the C-shaped tube length and joint location was studied by double shear tests. The effects of preload and concrete spray layer thickness on the roadway deformation and plastic zone were studied by numerical simulations. With the results of these studies, ACC supporting design methodology was proposed and conclusions are drawn as follows:

- (1) Increasing C-shaped tube length can reduce slip state length. Before C-shaped tubes reach joints, C-shaped tube length only affects slip state length. After the C-shaped tube length exceeds 15 cm beyond the joint, continuing to increase the C-shaped

tube length has no effect on the joint peak shear strength and only increases the shear strength during shear.

- (2) ACC and concrete spraying layer can form a stable extruded arch structure, so that the broken and soft rock within the loosen zone is in triaxial-stress state, effectively raising surrounding rock properties and controlling its deformation. On this basis, increasing the preload applied to ACC can effectively control the horizontal displacement of the roadway.
- (3) Based on the research results on ACC preload, C-shaped tube length, and concrete spray layer thickness, the ACC support design method is proposed, and the ACC support parameter selection methods are clarified.

Data Availability

All the data, models, or codes that support the findings of this study are available from the corresponding author upon reasonable request.

Conflicts of Interest

The authors state there are no conflicts of interest regarding the publication of this paper.

Acknowledgments

The authors would like to thank the Natural Science Foundation of China (No. 51474218) for providing financial support.

References

- [1] R.-L. Shan, X. Kong, Z. Wei, and M. Li, "Theory and application of strong wall support in coal roadway," *Chinese Journal of Rock Mechanics and Engineering*, vol. 31, no. 8, pp. 1305–1315, 2013.
- [2] J. Chen, S. Saydam, and P. C. Hagan, "Numerical simulation of the pull-out behaviour of fully grouted cable bolts," *Construction and Building Materials*, vol. 191, pp. 1148–1158, 2018.
- [3] Y.-L. Du, "Study on pull-out bearing characteristics of bolts with different bonding lengths," *Journal of mining and strata control engineering*, vol. 3, no. 3, pp. 5–12, 2021.
- [4] H.-J. Su, "Study on mechanical properties of rock mass with built-in rough joints based on 3D printing," *Journal of mining and safety engineering*, vol. 37, no. 3, pp. 840–846, 2021.
- [5] D.-P. Xu, Q. Jiang, S.-J. Li, S.-L. Qiu, S.-Q. Duan, and S.-L. Huang, "Safety assessment of cable bolts subjected to tensile loads," *Computers and Geotechnics*, vol. 128, Article ID 103832, 2020.
- [6] H.-H. Yuan, "Tunnel stability control in the high stress area below the coal wall in the mining area," *Safety In Coal Mines*, vol. 47, no. 10, pp. 173–177, 2014.
- [7] X.-L. Cheng, "Study on deformation and failure characteristics and control technology of surrounding rock in deep shaft gob driving roadway," *Journal of mining and safety engineering*, vol. 38, no. 2, pp. 227–238, 2021.
- [8] Z.-Z. Xie, "Study on principle and application of cross-border anchorage in thick layer of coal roadway roof," *Chinese Journal of Rock Mechanics and Engineering*, vol. 40, no. 6, pp. 1195–1208, 2021.
- [9] N.-J. Ma, "Mechanism of butterfly-type impact ground pressure occurrence in homogeneous circular roadways and its determination criteria," *Journal of China Coal Society*, vol. 41, no. 12, pp. 2678–2689, 2016.
- [10] W.-P. Huang, *Research on Asymmetric Deformation Mechanism of Deep Shaft Roadway and Control of Surrounding Rock Rheology and Disturbed Deformation*, China University of Mining and Technology, Beijing, China, 2012.
- [11] F. Pellet and P. Egger, "Analytical model for the mechanical behaviour of bolted rock joints subjected to shearing," *International Journal of Rock Mechanics and Rock Engineering*, vol. 31, no. 7, pp. 73–97, 1996.
- [12] H. Jia, Y. Wang, S. Liu et al., "Experimental study of stirring and resin-blocking devices for improving the performance of resin-anchored cable bolts," *Rock Mechanics and Rock Engineering*, vol. 54, no. 8, pp. 3995–4008, 2021.
- [13] Q. Gong, F. Wu, D. Wang, H. Qiu, and L. Yin, "Development and Application of cutterhead working status monitoring system for shield TBM tunnelling," *Rock Mechanics and Rock Engineering*, vol. 54, no. 4, pp. 1731–1753, 2021.
- [14] S.-P. Liu, K. Gu, C. Zhang, and B. Shi, "Experimental research on strain transfer behavior of fiber-optic cable embedded in soil using distributed strain sensing," *International Journal of Geomechanics*, vol. 21, no. 10, 2021.
- [15] E. Jahangir, L. Blanco-Martín, F. Hadj-Hassen, and M. Tijani, "Development and application of an interface constitutive model for fully grouted rock-bolts and cable-bolts," *Journal of rock mechanics and geotechnical engineering*, vol. 13, no. 4, pp. 811–819, 2021.
- [16] D. Li, M. Cai, and H. Masoumi, "A constitutive model for modified cable bolts exhibiting cone shaped failure mode," *International Journal of Rock Mechanics and Mining Sciences*, vol. 145, Article ID 104855, 2021.
- [17] A.-l. Zhang, T.-y. Liu, Y.-x. Zhang, X.-c. Liu, and Z.-q. Jiang, "Experimental and numerical research on mechanical behavior of prestressed high-strength bolt joint," *Journal of Constructional Steel Research*, vol. 182, Article ID 106690, 2021.
- [18] H.-S. Jia, D. He, S. Liu, and M. Fu, "Experimental study of an orientation and resin-lifting device for improving the performance of resin-anchored roof bolts," *Rock Mechanics and Rock Engineering*, vol. 51, no. 3, pp. 211–231, 2020.
- [19] H.-H. Yuan, *Study on Shear Anchor Pipe Cable Support in Layered Surrounding Rock Roadway*, China University of Mining and Technology, Beijing, China, 2020.
- [20] R. Shan, Y. Bao, P. Huang, W. Liu, and G. Li, "Study on double-shear test of anchor cable and c-shaped tube," *Shock and Vibration*, vol. 2021, Article ID 9948424, 10 pages, 2021.
- [21] R. Shan, S. Zhang, P. Huang, and W. Liu, "Research on full-section anchor cable and C-shaped tube support system of deep layer roadway," *Geofluids*, vol. 2021, Article ID 5593601, 13 pages, 2021.
- [22] J.-K. Yuan, C. Ye, J. Yang et al., "Experimental and numerical investigation on the deterioration mechanism for grouted rock bolts subjected to freeze-thaw cycles," *Bulletin of Engineering Geology and the Environment*, vol. 80, no. 7, pp. 5563–5574, 2021.